

Using Rotordynamics to Solve Serious Machinery Vibration Problems

Malcolm E. Leader, P.E.
Applied Machinery Dynamics Co.
P.O. BOX 157
Dickinson, TX 77539
MLeader@RotorBearingDynamics.COM

Abstract: Seven case histories show how applying lateral and torsional rotordynamics analyses can solve serious machinery problems. In the first lateral case history a centrifugal compressor rotor critical speed is located exactly on operating speed. New bearings are designed that are significantly softer and the rotor mass is increased by one-third. These two modifications reduce the critical speed well below operating speed and greatly reduce the sensitivity to imbalance. In the second lateral case history a gas turbine is unstable with very high subsynchronous vibration. A special hybrid 3-pad dual pressure dam bearing is designed that is much more stable and less sensitive to clearance changes than the original 3-lobe bearings. In the last lateral case history a damper bearing is applied to a steam turbine rotor in order to decrease the effective bearing stiffness and allow for the damping to control the critical speed. Four torsional case histories explore ways to solve torsional vibration problems through proper design and system modifications.

Key Words: Bearings; Critical Speeds; Damping; Design; Fatigue; Forced Response; Instabilities; Modeling; Properties; Rotors; Squeeze Film; Stability; Stress; Torsional; Vibration

Introduction: The rotordynamics modeling of rotating machinery has become a relatively mature science in the past 30 years. While many different mathematical techniques have been applied including matrix transfer and polynomial expansion, the use of finite element modeling techniques has allowed for faster and more realistic system modeling. This paper will show how some of these techniques are applied including the ability to analyze complete coupled trains where flexible couplings connect two or more rotors. In the past couplings were included as lumped masses and inertias. Although the flexible parts of modern couplings do somewhat isolate rotors laterally from one another, there are some dynamic effects that are transmitted through these couplings. In case 1 the coupling played an integral part in the compressor rotor's dynamics.

The ability to include substructures such as bearing housings, casings, flexible supports and foundations has greatly improved the accuracy of rotordynamics analysis. In case 2 in this paper, an aero-derivative gas turbine had a very complex substructure. Without a concentrated effort to include all of the elements of the casing and foundation, the problem could not have been solved. Extensive modal testing was used in this case to get effective stiffness and mass properties but finite element modeling of structures can also be used to determine these properties.

One of the biggest gains in the last decade for rotordynamics modeling and analysis is the production of very high quality graphics, some of which are displayed in this paper. Although it can't be shown on paper, animations have become a very useful tool to help visualize the dynamic behavior of rotor bearing systems. It is especially useful as a learning tool or to convince a skeptical boss that the proposed fix is the right one.

There are three principal instances when a rotordynamics study is appropriate. The most obvious is to help resolve vibration problems that have resisted normal maintenance attempts such as balancing and alignment. Some machines just have design flaws or need improvement in order to withstand operational abuse such as surging or contaminant buildup. Six of the seven cases presented in this paper cover the analysis of problem machines and the applied measures to solve the vibration problems. The next appropriate time to seek out a rotordynamics analysis is when system modifications are planned. This might be changing coupling designs or it might involve a complete revamp, adding impellers or other modifications. The rotordynamics analysis can tell ahead of time if the modifications will cause any problems. The big advantage is that, in most cases, the baseline dynamic behavior of the machine is known and the model can be tweaked to match this known pattern. Finally, while most manufacturers apply competent rotordynamics analysis to their machinery, an independent analysis can be very cheap insurance. This will not only catch potential mistakes, but can lead to suggestions for improvements before the machine is manufactured. As Charlie Jackson explained to me when I went to work for him 30 years ago: "We're not going to install machinery problems." Case six is an example of this approach.

Case 1 - Fixing a Critical Speed Interference Problem

This case involves a three stage high speed refrigeration compressor with multiple problems that led to a very unreliable machine, numerous wrecks and a lot of expensive rebuilds and down time. A great deal of effort had been put into improving the compressor's reliability but the machine had actually gotten worse at time passed. One of the primary problems was that polymer would build up over time causing large imbalances on the rotor. Cleaning the polymer required removing the compressor to a shop for disassembly. Fortunately there was a spare compressor that could be swapped in place of the machine being rebuilt. The other major problem was that, due to process changes, the compressor was constantly surging. This was so bad that the displacement probes had long ago been removed from the compressor since they showed high vibration at all times. In many cases it was possible to actually see the compressor case motion during surge events.

Figure 1 is a photograph of the rotor. In an effort to understand the dynamics of this compressor a finite element model was created of the high speed part of the train as shown in figure 2.



Figure 1 - Photograph of Refrigeration Compressor Rotor

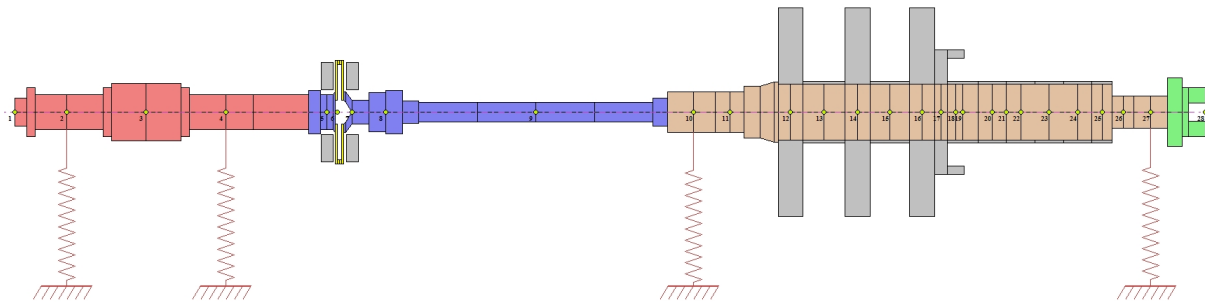


Figure 2 - Rotordynamics Model of Pinion, Coupling, and Compressor Rotor

It was necessary to model the entire high speed part of this train since the coupling is a quill shaft design and is essentially integral with the compressor shaft. A single flexible diaphragm connects to the pinion. While the pinion is essentially a stiff shaft without any interfering resonances, it completes this model for an accurate prediction of the rotordynamics. The compressor's three impellers are grouped at one end since this particular model can accommodate an additional two stages if required. This machine is driven by a motor through the speed increaser. The compressor runs at a constant speed of 15,200 RPM. The original bearings were pressure dam type as shown in figure 3.

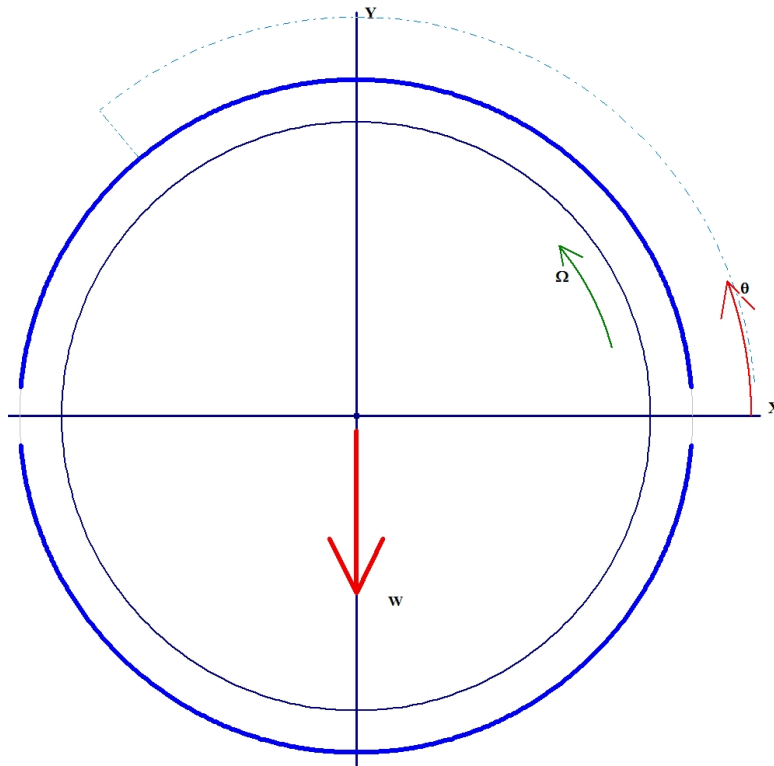


Figure 3 - Cross Section of Original Pressure Dam Bearing

Upon examination, the pressure dam bearings appeared to have been optimized for maximum effect from the pressure dam. Unfortunately, this made the bearings very stiff. It also places the first critical speed right on running speed. Figure 4 is a Bode plot of the predicted unbalance response to 16W/N imbalance placed at the compressor rotor center. Note the amplification factor of 19.2 indicating poor damping.

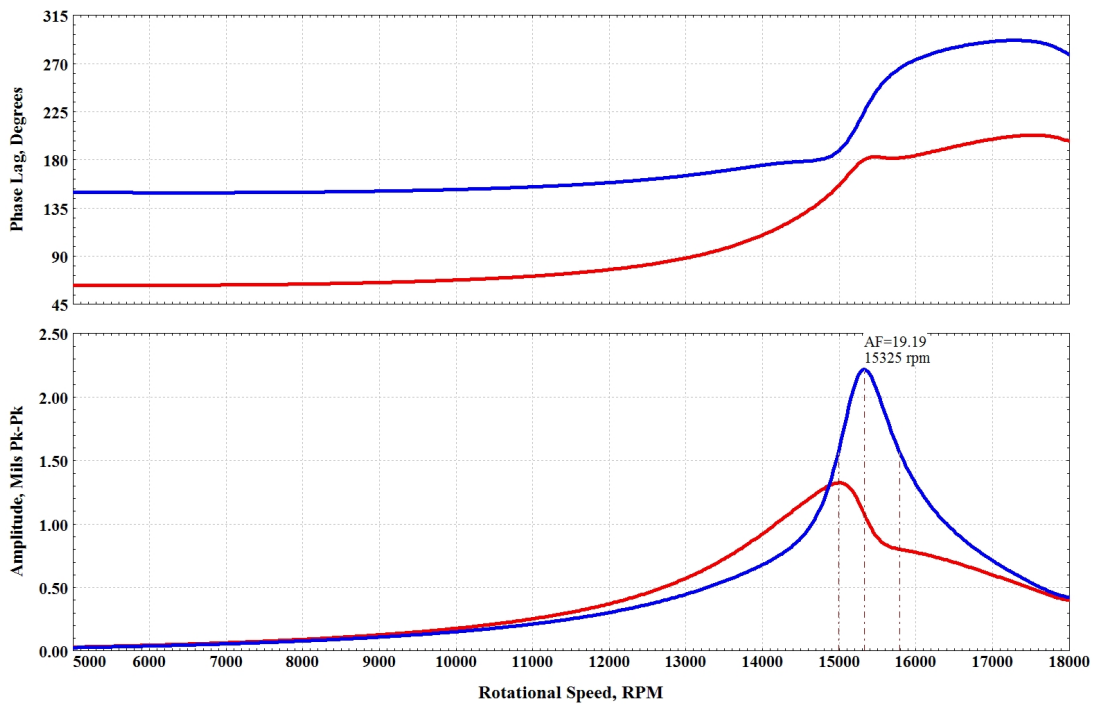


Figure 4 - Predicted Unbalance Response of Refrigeration Compressor

The initial attempt at improving the vibration response of this compressor was to redesign the bearings. There was only room for fixed profile type bearings and many designs were considered including other pressure dam configurations, 3 and 4-lobe designs, offset half, elliptical and plain bearings. It was determined that a 3-lobe design showed the most promise and an optimization process was completed that involved determining the best combination of all geometric variables including clearance, preload, pad offset and pad orientation. The preferred final design is plotted in figure 5.

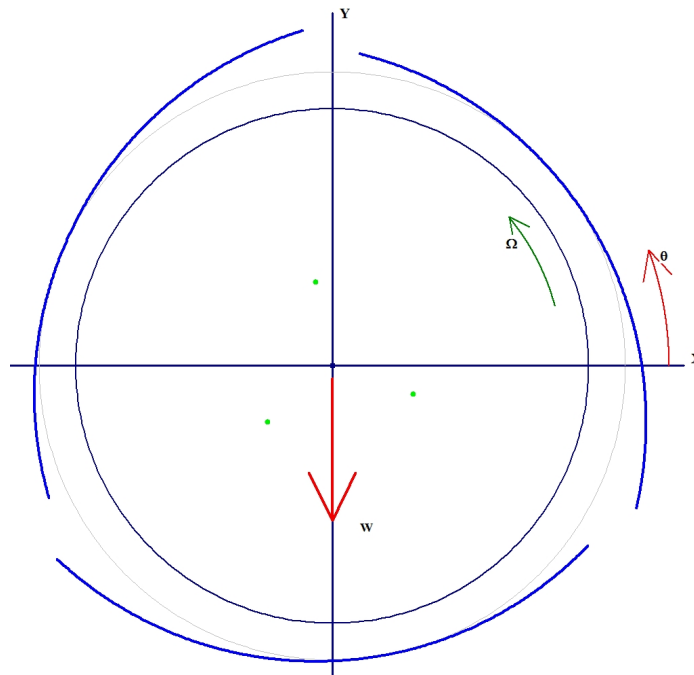


Figure 5 - Cross Section of Optimized 3-Lobe Bearing

At operating speed the effective dynamic stiffness of the original pressure dam bearing was 3.3 million LB/IN in the horizontal direction and 7.1 million LB/IN in the vertical direction. The 3-lobe bearing dynamic stiffness was determined to be 2.1million LB/IN in the horizontal direction and 2.2 million LB/IN in the vertical direction. The new predicted unbalance response with these bearings is plotted in figure 6.

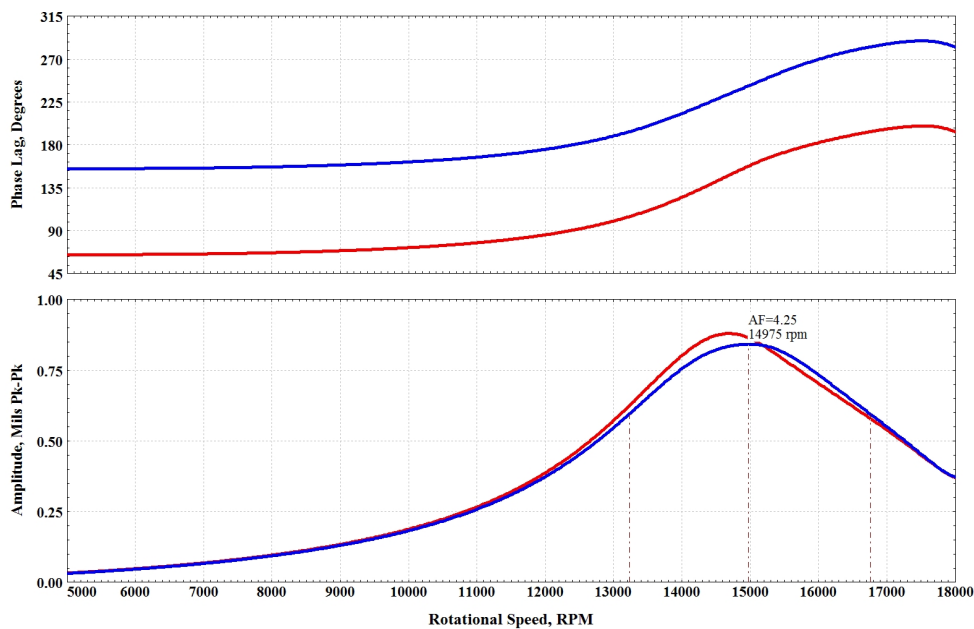


Figure 6 - Predicted Unbalance Response with 3-Lobe Bearings Only

While the new 3-lobe bearings reduce the critical speed amplitude and the amplification factor significantly, the critical speed frequency is still too close to operating speed. The best way to lower a critical speed frequency is to add mass. Since this machine had room for two additional impellers, adding a dummy impeller appeared to have high potential. The original rotor weighed only 102 pounds. The proposed disk, seen in figure 7 added another 34 pounds.

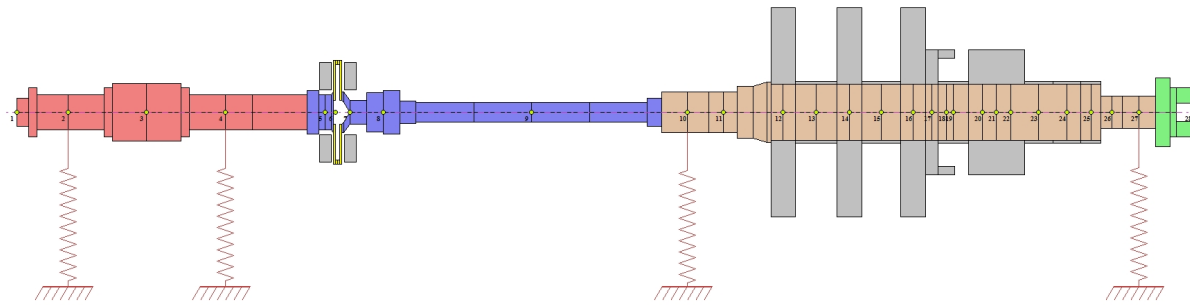


Figure 7 - Modified Compressor Rotor Model

This modification proved to be very effective. The predicted unbalance response, figure 8, with the dummy wheel and the optimized 3-lobe bearings shows very low amplitude (for the same 16W/N imbalance) and an amplification factor less than 2 which is close to critically damped.

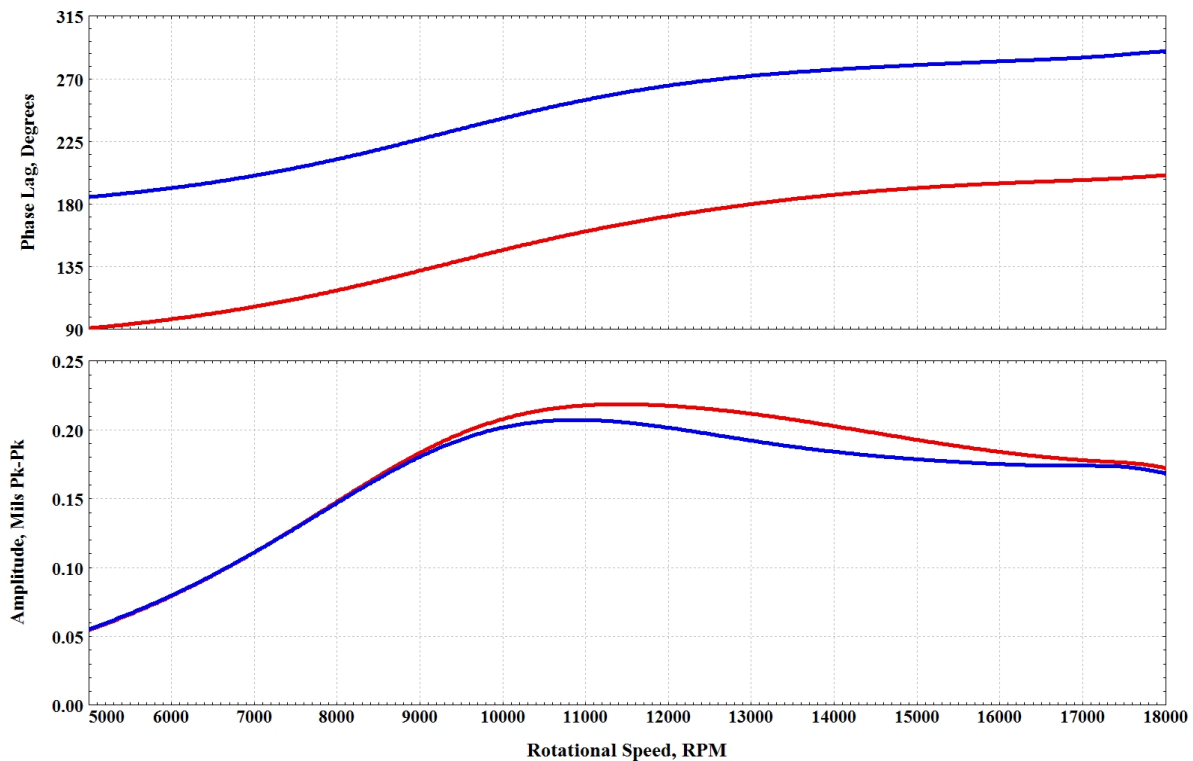


Figure 8 - Predicted Unbalance Response with 3-Lobe Bearings and Dummy Wheel

Thus, new bearings were manufactured and one compressor was rebuilt with a dummy wheel. This was installed and started. The reduction in vibration was remarkable. Polymer buildup no longer caused high synchronous vibrations. However, compressor surging continued and damaged the new bearings. To counter this, bearings were made of solid bronze and these are able to withstand the surging. To date with these fixes in place, the only reason for removing a compressor is when the polymer buildup becomes so severe that it blocks flow through the gas path. There is a significant ongoing effort to remove the solids from the gas stream but neither that issue nor the surging problem have been resolved. Once these issues are fixed, this machine should have very good long-term reliability.

UPDATE, 2008: The process problems have been eliminated and the machine is extremely smooth and vibration free.

Case 2 - Aero-derivative Gas Turbine Instability

Aero-derivative gas turbines are commonly used in the oil recovery business to run generators and pumps. The unit presented here had a history of violent instabilities near half running speed. The problem existed on some units even when new and would often appear and disappear without any logical reason that could be found. This type of machine has a relatively rigid rotor consisting of an axial air compressor section and a combustion section where the fuel is injected into the air and ignited. The hot expanding gas then passes through a 2-stage turbine section that powers the compressor. This part of the machine is often called the gas generator. The hot gas then powers a separate turbine that runs the driven machinery. A picture of the gas generator rotor in this case history is shown in figure 9.

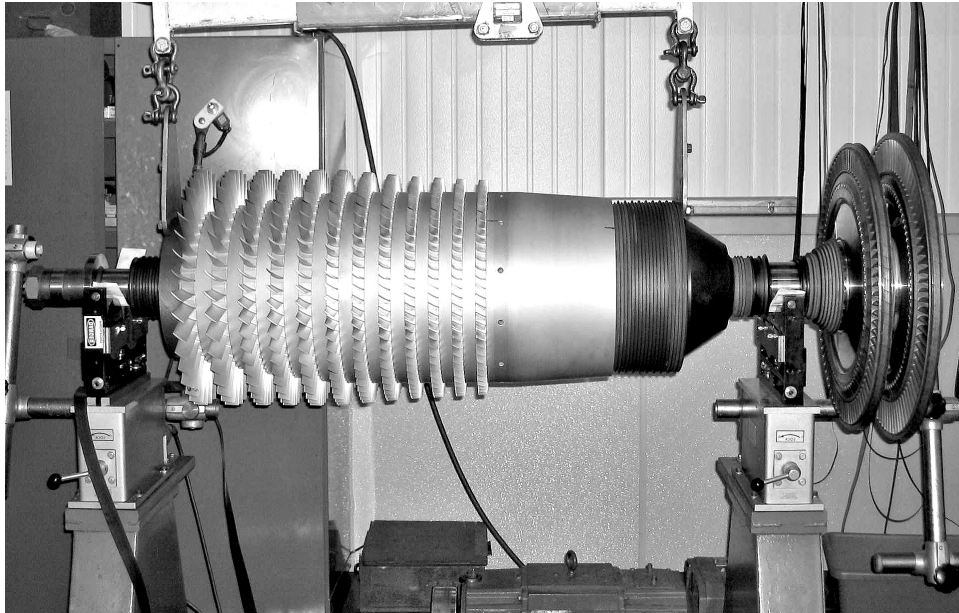


Figure 9 - Photograph of Gas Turbine Rotor

Note that there are radial holes just after the last stage of the compressor blading. These ports collect discharge air and channel it down the center of the shaft, through the journal area and out around the turbine disks for cooling purposes. This will be an important design consideration as the hot gas causes the bearing journal to grow about 5 mils in diameter from ambient to operating conditions. Thus, the clearance of this bearing is critical to achieving stable operation.

Constructing a finite element model of this machine was very complicated. If just the rotor is modeled, the calculated unbalance response isn't remotely like the measured vibrations and no instabilities are predicted. In a situation like this where the machine casing and support structure are fairly light, a substructure model was created based on actual weights and dynamic stiffnesses from modal testing. The final model, figure 10, is quite elaborate. The rotor is a multi-piece construction with two thru-bolts holding everything together. The case is shown surrounding the rotor and is as close as possible to the actual case. The bearings are shown as dark "boxes" between the rotor and case. Springs attach the casing to other boxes representing intermediate structural supports. These, in turn, are connected to ground. There are also links between structural elements representing the way the machine is connected and mounted. More than a month was spent developing this model. It was time well spent since the response predictions then matched field test data well.

There is a long labyrinth seal between the compressor and turbine sections. This can be seen in figure 9 and 10. It is believed that this seal was generating a great deal of the destabilizing cross coupling and a pseudo bearing was placed at this location so that various amounts of cross coupling could be added to the model for stability calculations. Some additional cross coupling was added to the rotor at the second turbine stage since Alford cross coupling forces are associated with turbine blading.

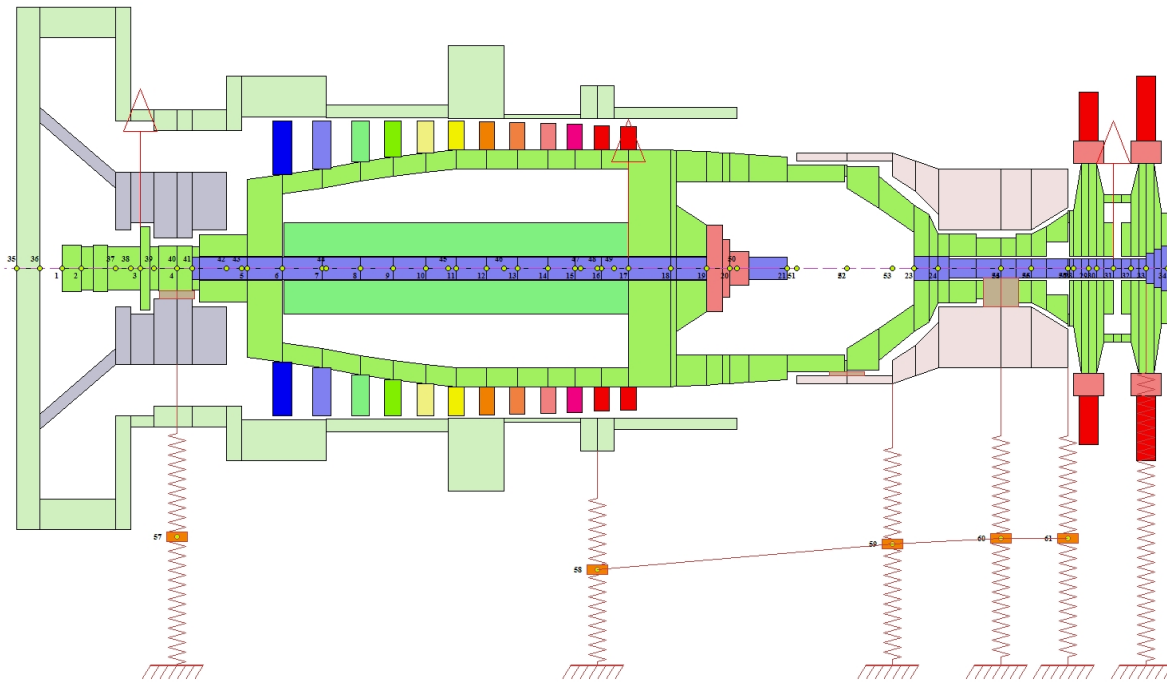


Figure 10 - Cross Section of Gas Turbine Rotor and Case Model

A typical rundown measurement taken in the field, figure 11, shows that there are several fairly well damped resonances. The first critical speed is the peak near 5,500 RPM and the second critical is near 8,000 RPM. Some of the other “bumps” are believed to be structural in nature.

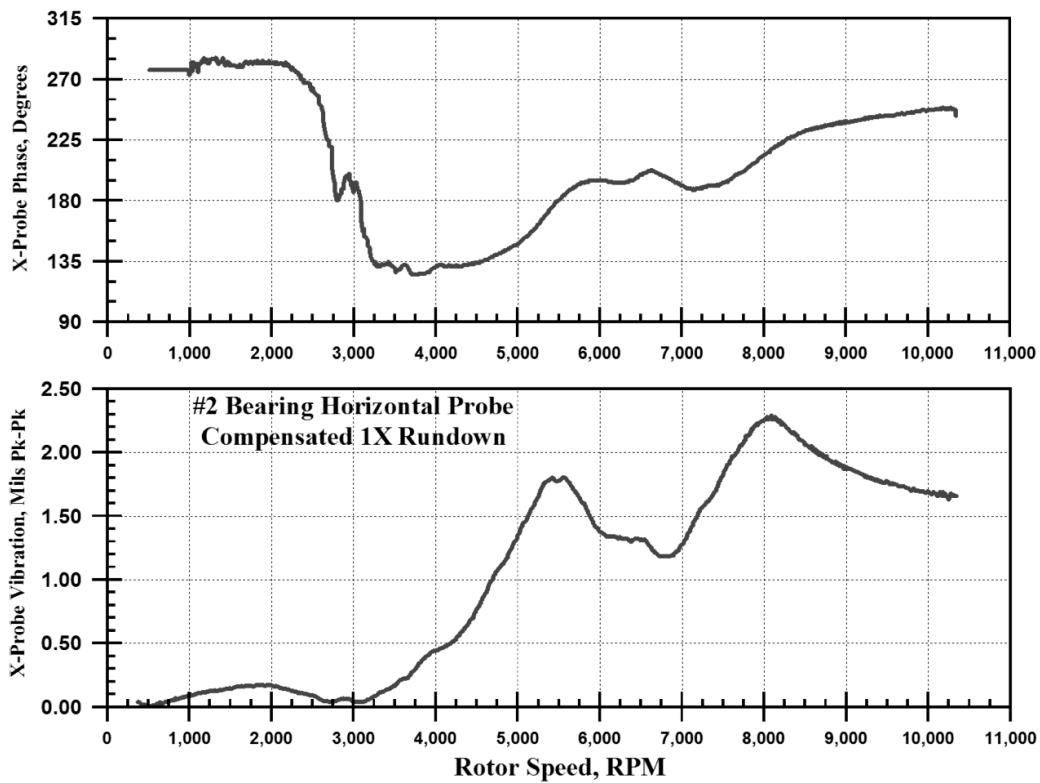


Figure 11 - Measured 1X Amplitude at Number 2 Bearing during Coastdown

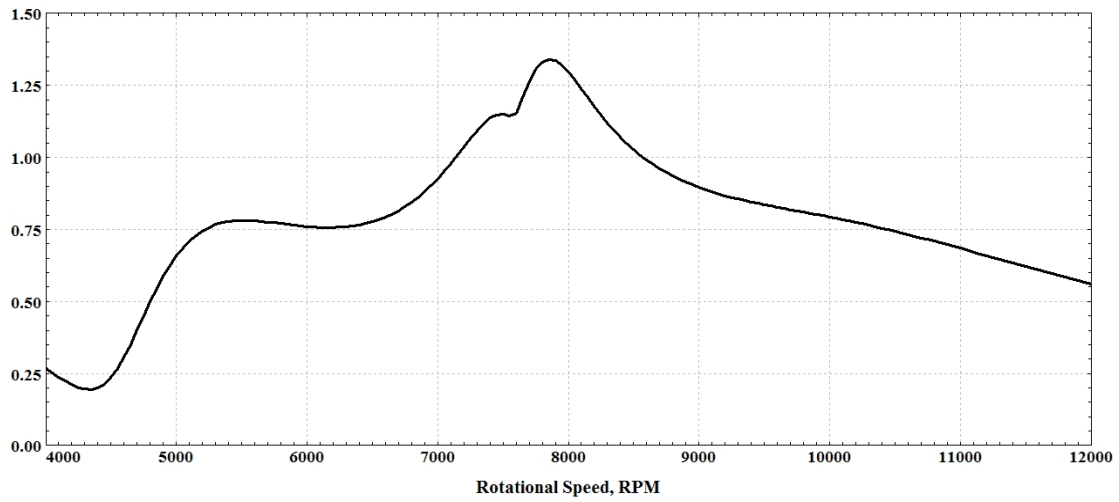


Figure 12 - Predicted Synchronous Response due to Imbalance at #2 Bearing

While this shows that the model is fairly accurate, it doesn't address the problem. Figure 13 shows a cascade plot of spectrums taken during a startup. A lot is going on in this plot, but the primary problem is the large subsynchronous vibrations above 10,000 RPM. These vibrations often exceeded 4 mils peak-to-peak. The instability is also clearly seen in the orbit plots as shown in figure 14.

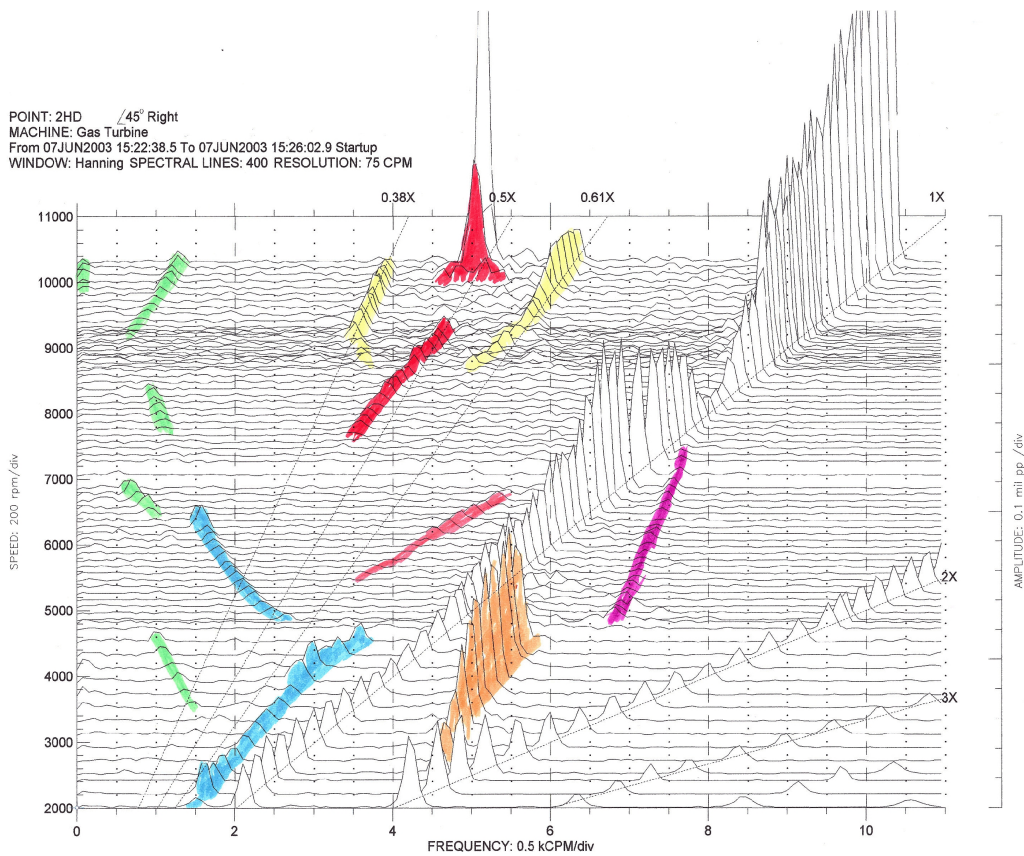


Figure 13 - Startup Cascade Plot from #2 Bearing Proximity Probe

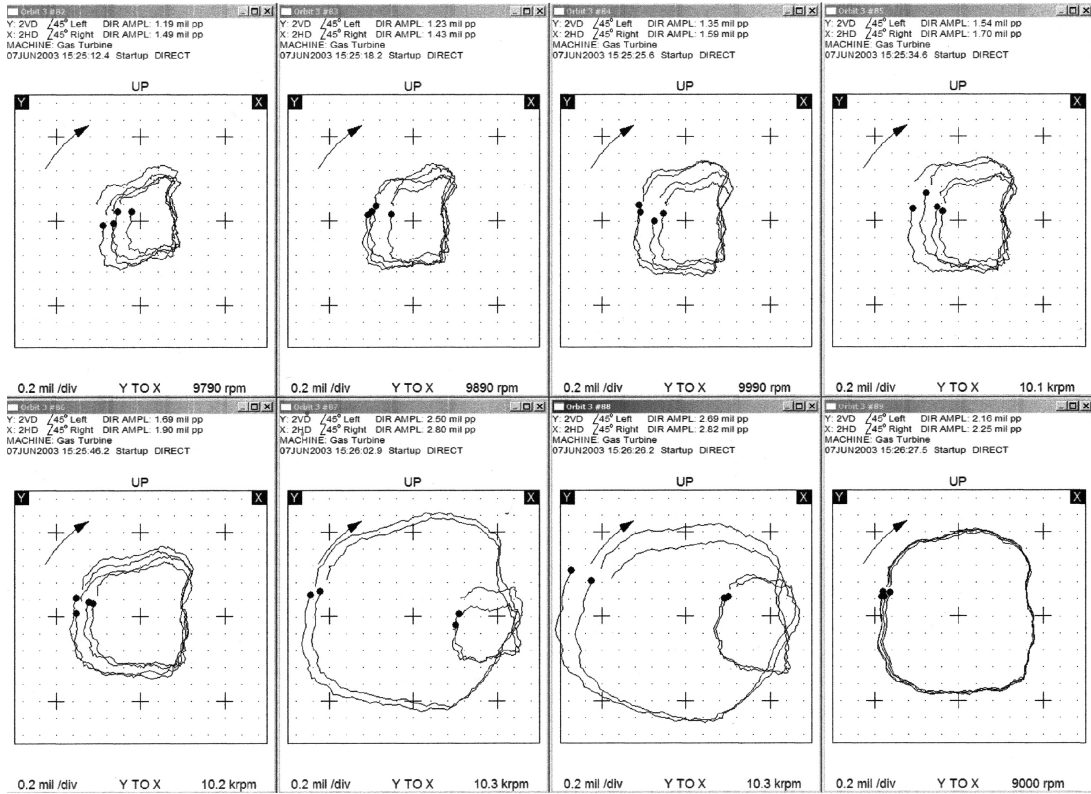


Figure 14 - #2 Bearing Orbits Showing 1/2X Vibrations

Although the experimental data suggests that a rub may be occurring, there was rarely any physical evidence that rubs had actually happened in most cases. This became an exercise in adding as much positive damping to the system without adding additional cross coupling. The only available option was a bearing design change. Since the bearing liners were very thin (less than 0.2 inches thick) a tilting pad bearing was not considered since the bearing housing was not able to be modified. Thus a complete survey of the various fixed profile bearings was completed and it was determined that a pressure dam bearing was significantly more stable than the original 3-lobe bearing. However, due to the thermal growth of the #2 journal, the bearing at this location must start with a diametral clearance of about 11 mils which then closes down to about 6 mils at operating conditions. After much work, a hybrid 3-pad, 2-pocket pressure dam bearing was conceived.

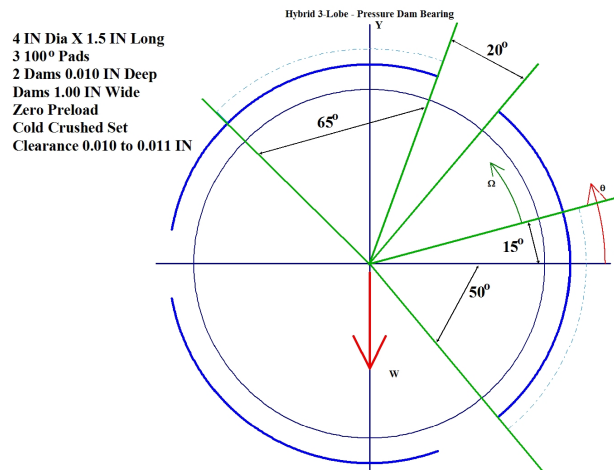


Figure 15 - Geometry of 2-Pressure Dam Bearing

This bearing, shown in figure 15 had just as good stability at the loose clearance as when the clearance was down to the normal 1.5 mils-per-inch journal diameter. Figure 16 is a plot of the calculated logarithmic decrement for this gas turbine with the original 3-lobe bearings, a single pressure dam bearing and the final dual pressure dam design.

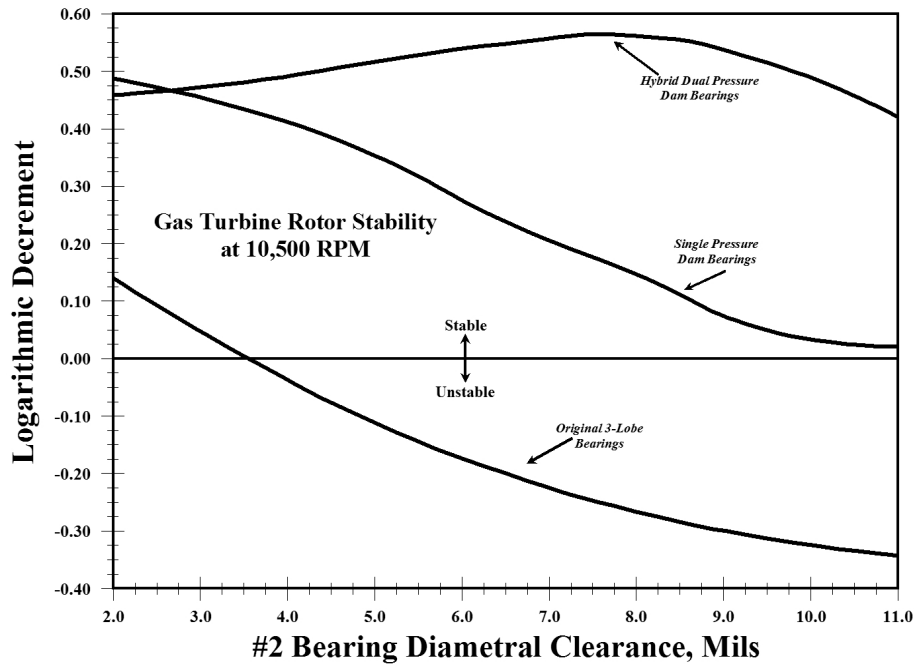


Figure 16 - Stability Comparison for Original 3-Lobe and Pressure Dam Bearings

Figure 17 shows that while there are some very small subsynchronous vibration components, there is nothing at $\frac{1}{2}X$ and the machine has been operated for several months at full speed and load without problems.

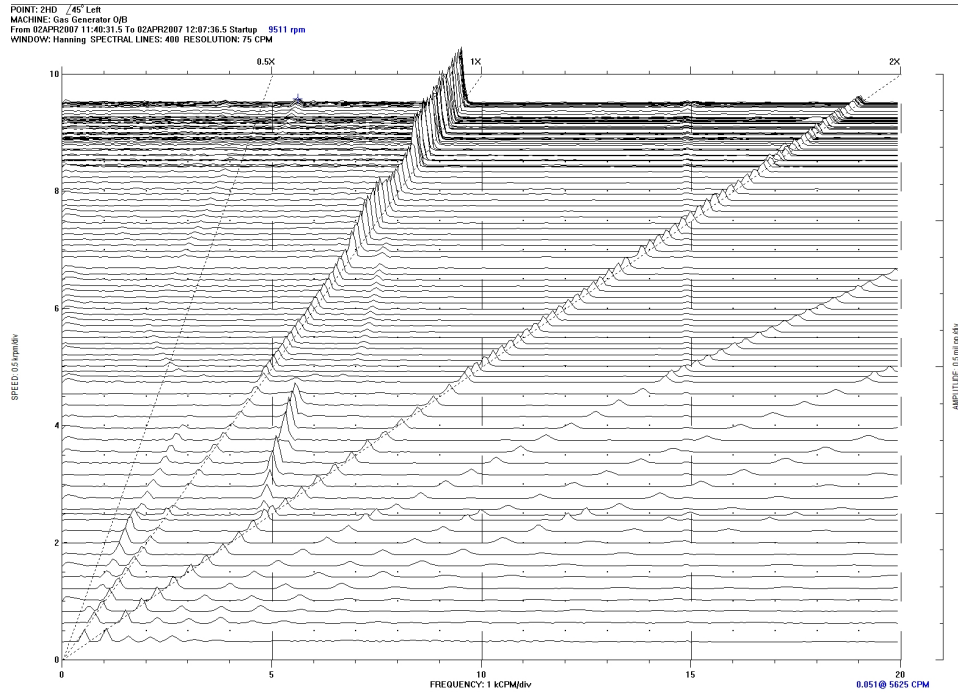


Figure 17 - Gas Turbine Startup Vibration at #2 Bearing with Dual Dam Design

Case 3 - Solving a Critical Speed Problem with a Damper Bearing

A turbine driven pump in a chemical plant was one of three supplying reactor cooling water. The other two pumps were motor driven with the turbine driven unit on slow-roll standby in case of a power failure. A complete loss of coolant would irreparably damage very expensive process equipment. Originally, only two pumps were required to meet demands, but soon production increases made running all three pumps imperative. Unfortunately, the old slow-roll standby turbine was very inefficient and costly to operate. Thus, a new multi-stage turbine was purchased and installed. The layout of this system is shown in figure 18.

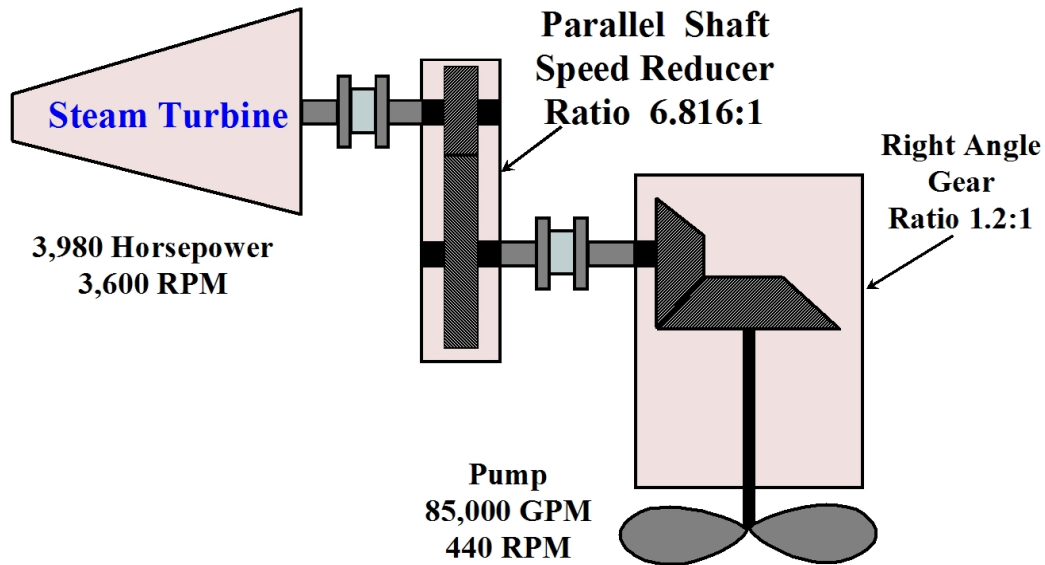


Figure 18 - Turbine Driven Coolant Pump System

Problems developed with the turbine almost immediately. High vibrations were observed while passing through the critical speed and often the proximity probe monitors were at such high levels that the alarms were all bypassed. Several times severe rubs occurred and the turbine had to be rebuilt numerous times. Despite very careful assembly, balancing and installation, numerous failures finally made the plant seek help with a redesign.

The most urgent question asked was how fast could a fix be implemented? With the turbine out-of-service and only the two motor driven pumps operating, a power failure could result in huge monetary losses. The first step was to measure the rotor and bearings and create a model. This was done quickly and the race was on to find a permanent redesign. Unfortunately, it soon became obvious that there was no easy fix. The existing bearings were 5 pad tilting pad load-on-pivot type that were about as good a design for this machine as you could apply. So, just changing bearings was unlikely to work.

Figure 19 is a mock-up of the turbine rotor as found. This design incorporates a compound Curtis stage wheel and up to 8 Ratteau stages depending on the horsepower requirements. Normal operating speed is 3,600 RPM. The undamped critical speed map, figure 20 reveals the problem. The bearing stiffness curves intersect the first critical speed up on the asymptotic part meaning that the shaft is too flexible or the bearings are too stiff. There wasn't time to even consider a stiffer shaft and softer bearings couldn't be found. The undamped mode shape, figure 21 shows that the bearings are nearly at node points

While there is no transient data available for this machine for the original condition, the predicted unbalance response showed a critical speed at 3,050 RPM with an amplification factor of 14.9 which means that there was very poor damping. The amplification factor, **A**, is related to the percent critical damping C_c by:

$$A = \frac{1}{2 C_c}$$

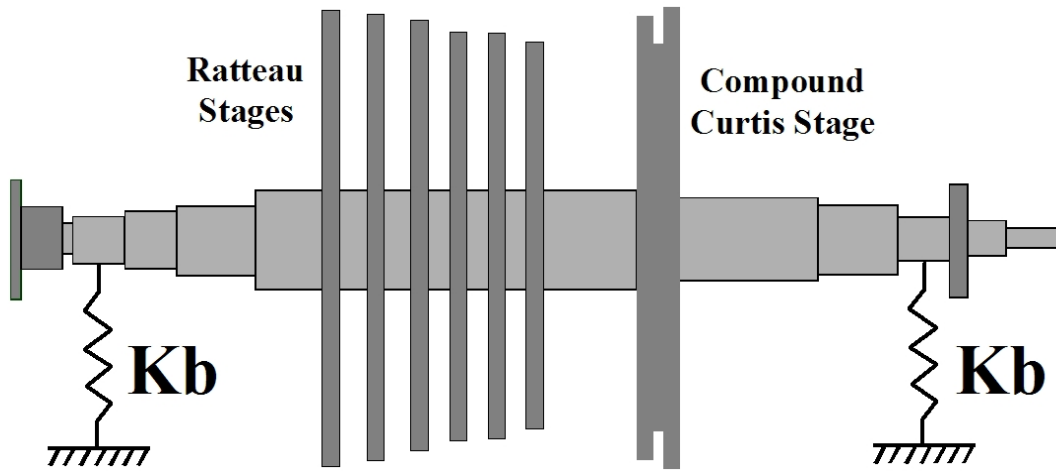


Figure 19 - Original Steam Turbine Rotor

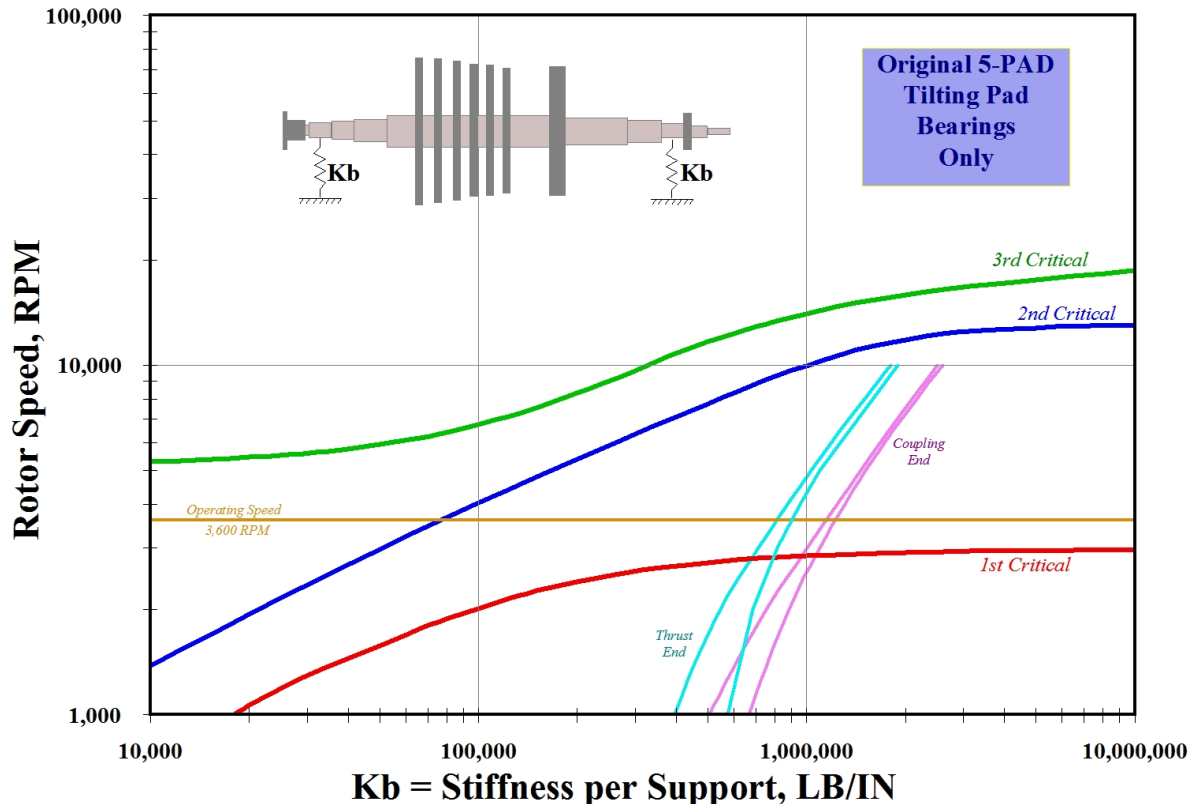


Figure 20 - Undamped Critical Speed Map of Original Steam Turbine Rotor

So, the original design had just 3.4 percent of critical damping available. It isn't surprising that the turbine had such maintenance problems. Just before the last rebuild, some brave technician measured 60 mils on the bearing housing during an aborted startup. The situation appeared fairly hopeless until Dr. John Nicholas suggested we look into a squeeze film damper design. Dr. E. J. Gunter also assisted with the conceptual part of the design.

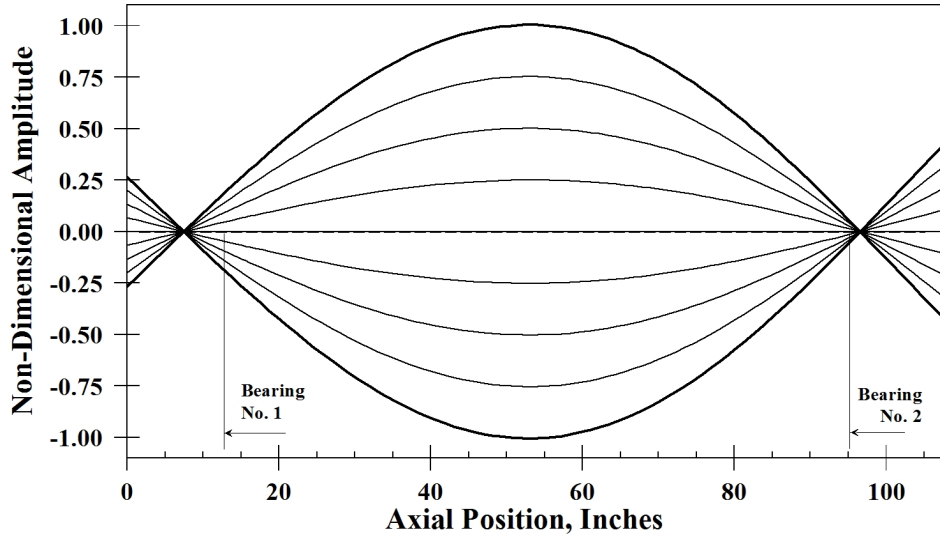


Figure 21 - Undamped First Critical Speed Mode Shape with Original Bearings

After some discussion it was decided to apply squeeze film dampers to the bearings. Fortunately there was plenty of room to do this in this machine. A squeeze film damper is simply a non-rotating thin annulus of oil surrounding the regular bearing as shown in figure 22. This film is only about 10 mils thick and o-rings are used as end seals. When the rotor moves laterally, the oil is displaced causing vibration energy to be absorbed.

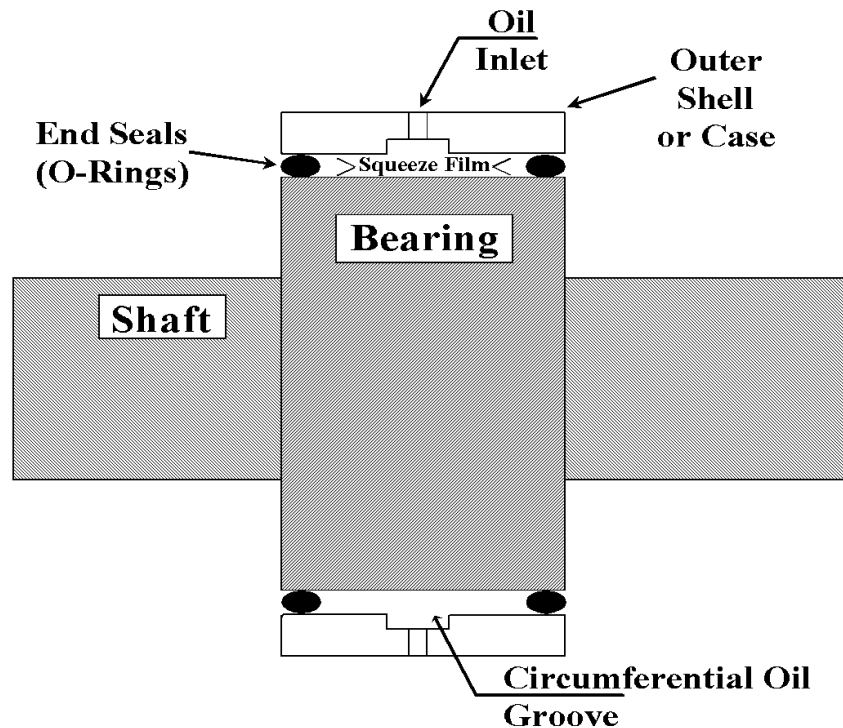


Figure 22 - Cross Section of a Squeeze Film Damper

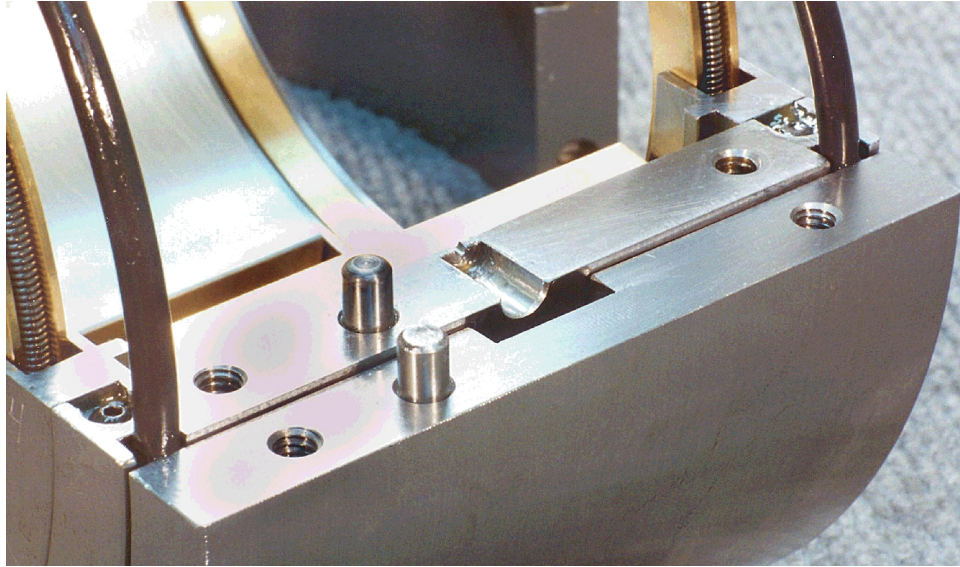


Figure 23 - Photograph of the Squeeze Film Damper Bearing

One of the tricks of designing this type of squeeze film damper is that the o-ring grooves must be offset eccentric with the bore so that when the rotor load is applied, the damper is centered in the annulus. This requires that the stiffness of the o-rings is known. For this case, a simple load deflection device was used to measure the stiffness of the o-rings. The stiffness and damping properties of the squeeze film damper itself are easy to calculate from closed form equations.

$$K = \frac{2 \mu R L^3 \varepsilon \omega}{c^3 (1-\varepsilon^2)^2}$$

and

$$C = \frac{\pi \mu R L^3}{2 c^3 (1-\varepsilon^2)^{3/2}}$$

Where ω is frequency in RAD/SEC, μ is dynamic viscosity in Reyns, ε is the eccentricity ratio, π is 3.14159... R is the damper radius, L is the damper length, and c is the damper radial clearance, all in inches. It is interesting to note that the damper coefficients are strongly dependent on clearance and length. It is important to not over design a damper or it won't work well.

Once the damper coefficients are calculated, the net system stiffness and damping must be calculated by combining them using the following equations.

Equivalent Stiffness

$$K_{Eq,xx} = \frac{\hat{K}_{sx} K_{xx} (\hat{K}_{sx} + K_{xx}) + \omega^2 (K_{xx} C_{sx}^2 + \hat{K}_{sx} C_{xx}^2)}{(\hat{K}_{sx} + K_{xx})^2 + \omega^2 (C_{sx} + C_{xx})^2}$$

AND

$$C_{Eq,xx} = \frac{K_{xx}^2 C_{sx} + \hat{K}_{sx}^2 C_{xx} + \omega^2 C_{sx} C_{xx} (C_{sx} + C_{xx})}{(\hat{K}_{sx} + K_{xx})^2 + \omega^2 (C_{sx} + C_{xx})^2}$$

WHERE:

$$\hat{K}_{sx} = K_{sx} - M_{sx} \omega^2$$

xx = Oil Film sx = Damper

In addition to the new damper bearing, dummy disks were added to the rotor in order to lower the first critical speed. More mass also makes the rotor less sensitive to wet steam upsets which were known to have occurred with some regularity. The modified rotor is shown in figure 24.

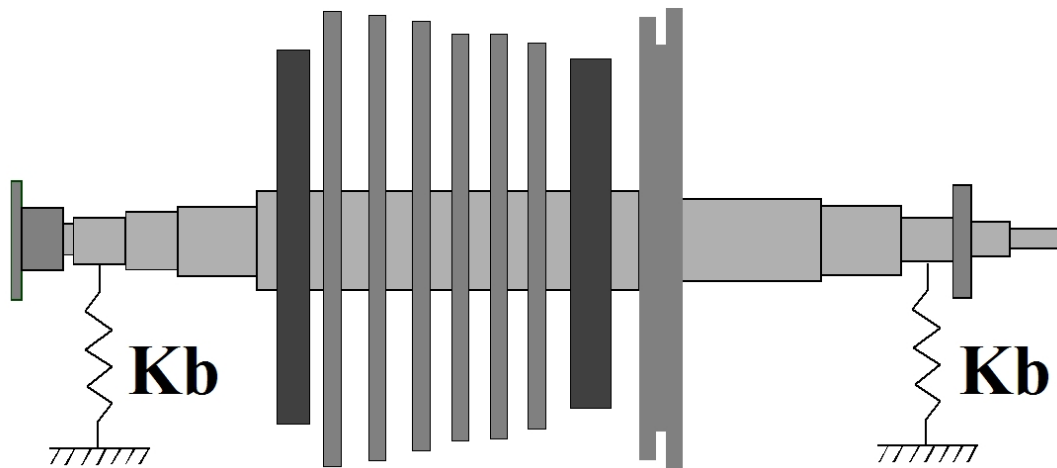


Figure 24 - Steam Turbine Rotor Modified with Dummy Disks

The original bearings, by themselves had a stiffness of about 1 million LB/IN and damping of about 2,000 LB-SEC/IN. Combined with the squeeze film damper the effective stiffness drops to 200,000 LB/IN and the damping drops to 1,000 LB-SEC/IN. So, even though the damping is cut in half, the dramatic drop in stiffness means that this damping is much more effective. The first critical speed mode shape with the damper installed is shown in figure 25. There is much more relative amplitude at the bearings and much less shaft deflection.

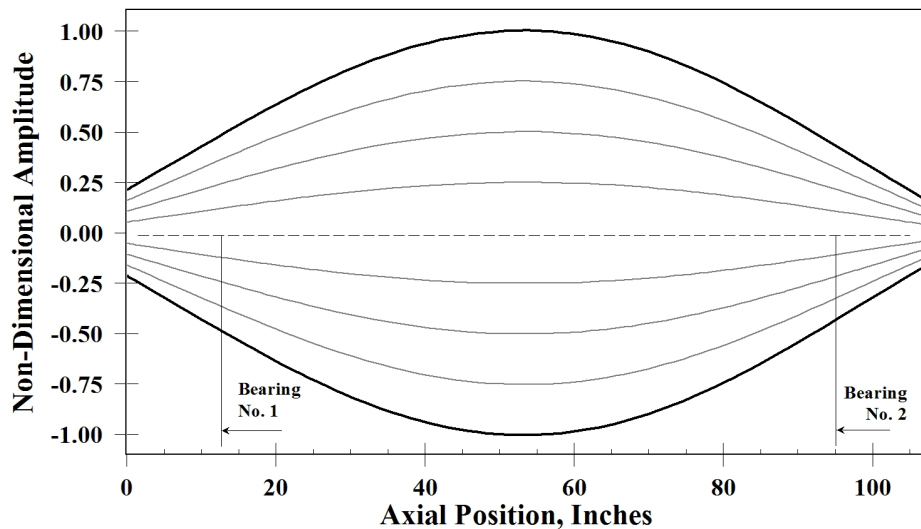


Figure 25 - First Critical Speed Mode Shape with Damper Bearing

Figure 26 is a comparison of the predicted unbalance response with the original bearings and no added disks and the revised design with dummy disks and the new squeeze film dampers installed.

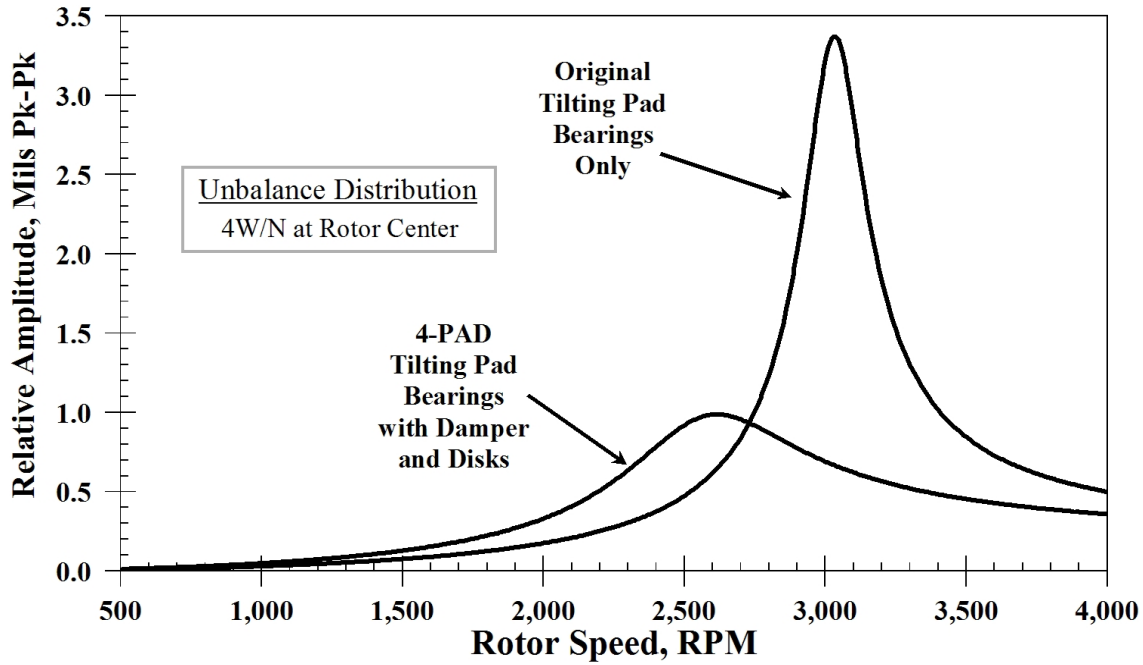


Figure 26 - Unbalance Response Comparison for Steam Turbine Rotor with Damper Bearing

The entire analysis process, testing of the o-rings, fabrication of the bearings and installation of the rebuilt turbine took only *10 days*. A lot of people cooperated and put in long hours to accomplish this feat. When the turbine was restarted, the measured vibration during startup was nearly exactly as predicted. Figure 27 shows that the amplification factor has been reduced from 14.9 to 4.4 and the critical speed has been lowered from 3,050 RPM to 2,600 RPM.

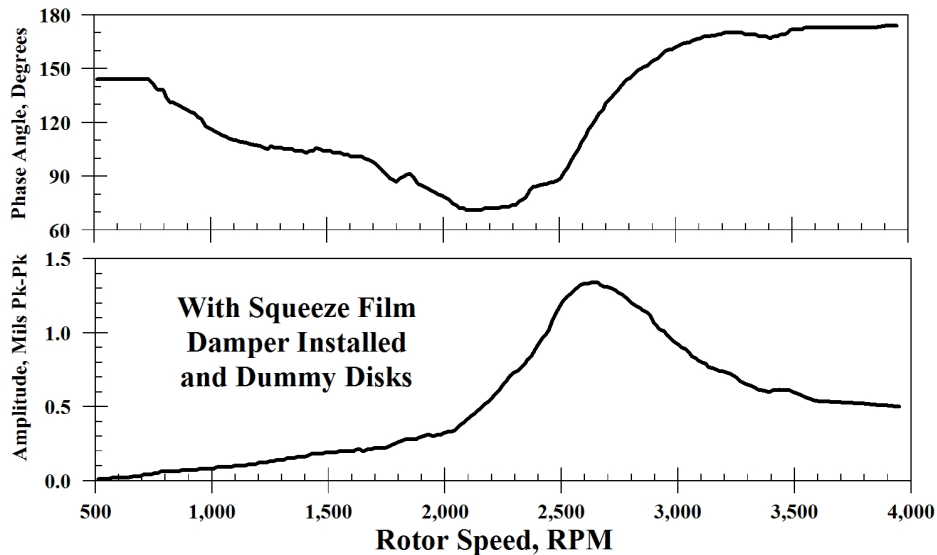


Figure 27 - Startup Bode Plot from Modified Steam Turbine

This machine has now operated for over 8 years on the original damper bearings without any problems other than routine maintenance and inspections. Even the monitoring system alarms are functioning.

PART 2 - EXAMPLE TORSIONAL ANALYSES

Four torsional examples are presented. All are based on actual industrial installations where unusual vibrations or failures were not solved by the typical route of balancing, alignment and operational adjustment. In many cases the problems lingered for many years before the torsional analysis revealed the underlying cause of the problems. The simplest type of torsional system is a driver and a driven like a turbine driving a fan or a motor driving a pump through a flexible coupling. The severity of any torsional problem is determined by the effect a torsional resonance is having on operational availability and maintenance.

Case 4 - Changing the Excitation Mechanism to Avoid Torsional Vibration

The simple 2-mass system illustrated in case 4 is an induction motor driving a centrifugal pump as indicated in figure 28. This is a typical API type process pump in light hydrocarbon service. The operating speed is 1,775 RPM and impeller has 3 vanes. Pressure pulsations from the impeller occur at 3X or 5,325 CPM.

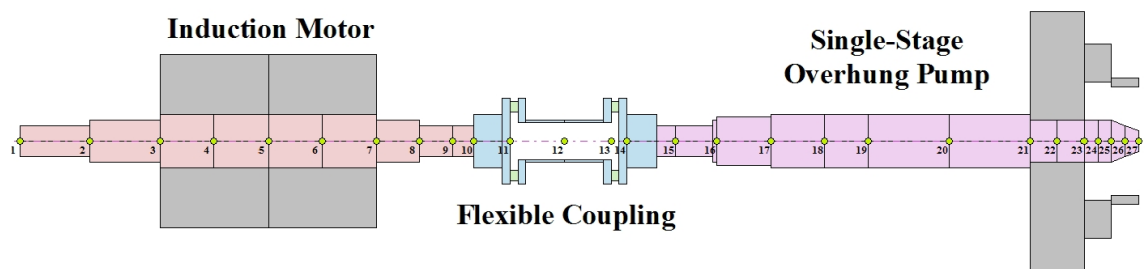


Figure 28 - Simple 2-Mass Torsional Motor-Pump Train

High vibrations on this train were detected at vane-pass frequency. Modifications to the pump including the “A” and “B” gaps and piping had little effect on reducing the 3X vibrations. A torsional analysis indicated that the first torsional resonance was 5,300 CPM. It was not possible to increase or decrease the coupling torsional stiffness enough to move the torsional resonance more than 100 CPM. The solution was to purchase a new impeller with 4 vanes moving the pressure pulsations well above the torsional resonance. The modified train ran smoothly after the impeller change and the seal and bearing failures were significantly reduced.

Case 5 - Changing the Couplings to Avoid Torsional Vibration

A basic geared system is illustrated by the turbine driven induced-draft fan train shown in figure 29. This train exhibited severe gear wear causing the gears to be replaced every 14 to 18 months. Many “fixes” were implemented including precision component balancing and hot alignment. These efforts did not decrease the failure rate. Finally, based on the gear manufacturer’s recommendation, a torsional analysis was conducted after it was found that the original design effort had ignored this aspect.

The gear ratio for this train was a 5.97:1 speed decrease. The torsional analysis revealed an unusual problem. The first torsional resonance was found to be coincident with the fan speed (750 to 770 RPM) and the second torsional resonance was found to be at the turbine speed of 4,480 to 4,600 RPM. The couplings were examined for possible modification and it was determined that stiffening the couplings would have no significant influence on the torsional resonances. Instead, the torsional stiffness of each coupling was reduced to give the necessary separation margin. Table 1 is a summary of the findings.

| Coupling Stiffness IN-LB/RAD | 1st Torsional Resonance (CPM) Separation Margin (%) | 2nd Torsional Resonance (CPM) Separation Margin (%) |
|--|---|---|
| <u>Original</u> L.S. 75.2 X 10 ⁶ H.S. 16.6 X 10 ⁶ | 760 CPM (None) | 4,540 CPM (None) |
| <u>Modified</u> L.S. 33.1 X 10 ⁶ H.S. 5.02 X 10 ⁶ | 647 CPM (12.6%) | 3,872 CPM (12.4%) |

Table 1 - Summary for Case 5 - Turbine-Gear-Fan Torsional Resonances

Once both couplings were replaced the system vibration dropped from near 0.5 IPS to less than 0.1 IPS and there has been no significant gear deterioration for over five years.

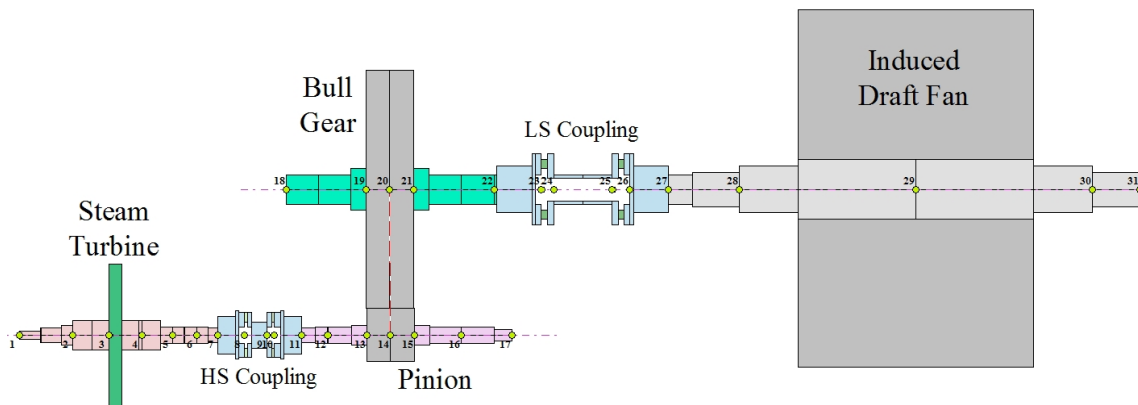


Figure 29 - Turbine Driven Induced Draft Fan Train

Case 6 - Designing the System to Accommodate Torsional Excitation and Stress

One of the most severe examples of transient torsional excitation occurs during the start of a synchronous motor. Case 6 (figure 30) consists of a 6-pole 5,500 HP synchronous motor driving an air compressor through a gear speed increaser. In this case torsional problems were eliminated in the design stage.

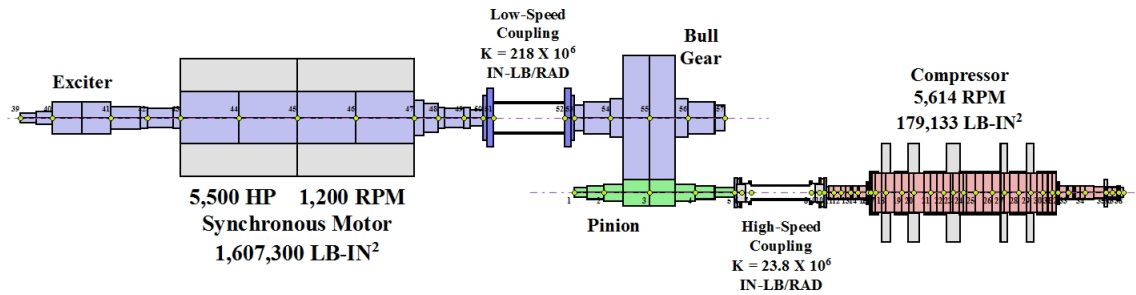


Figure 30 - Synchronous Motor-Gear-Compressor Train

Every synchronous motor generates alternating torque impulses during a startup. These pulses begin at twice line frequency (7,200 CPM in the US) and decline inversely with speed to zero when synchronous speed is attained. This means that every torsional resonance between 0 and 7,200 CPM will be excited during each startup. These torque pulsations are not trivial and have been the cause of many machinery failures. Thus, any machine train with a synchronous motor must be evaluated with a transient torsional analysis. A transient analysis consists of creating a spring-mass model and defining all the torque producers and absorbers. The torque information is generally available only from the motor vendor who must communicate with the manufacturer of the other machinery and produce a set of torque curves similar to figure 31. A forced response procedure is applied to the model simulating the startup. At time zero, the driving, oscillatory, and load torques are applied simultaneously. This causes the train to accelerate in speed. Then, at very small time steps, a new speed is calculated along with the torsional oscillation amplitude. Ultimately, the alternating torque amplitudes are converted to the shear stresses in the shafts. One important calculation coming from this analysis is the time to reach full speed as seen in figure 32. Anything over 20 seconds could be damaging to the motor. After synchronization, the motor torque is balanced by the load torque and there are no more alternating torque pulsations from the motor. Very low frequency oscillations often seen immediately after synchronization are due to interaction of the mechanical system with the electrical grid.

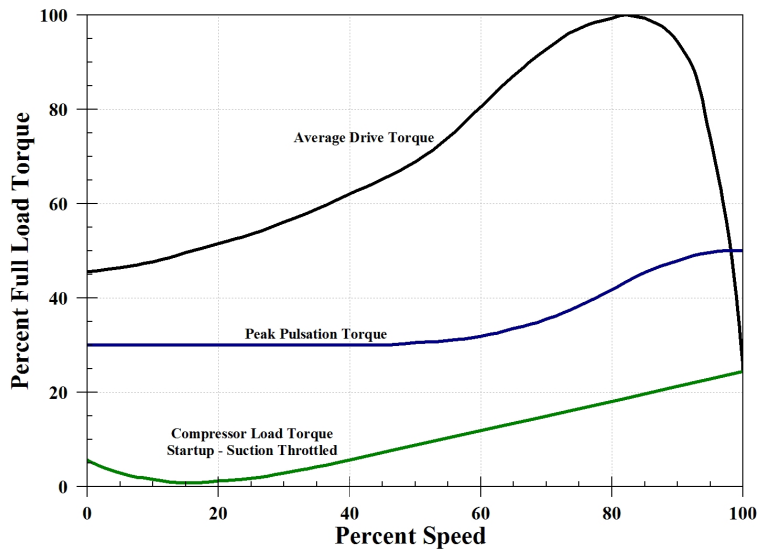


Figure 31 - Speed vs. Torque Curves for 5,500 HP Synchronous Motor

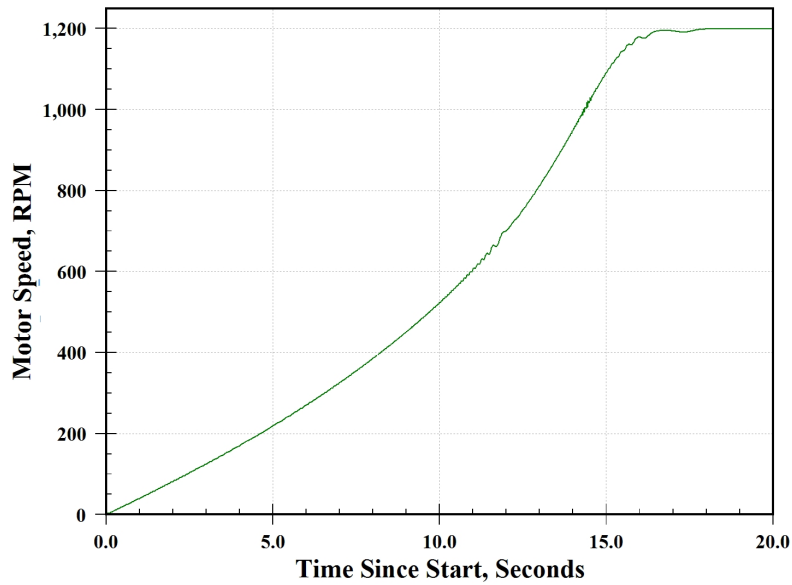


Figure 32 - Startup Time Calculation for Synchronous Motor-Gear-Compressor Train

Ripples in the time-speed curve of figure 32 are actual speed fluctuations due to the torsional resonances. The first resonance encountered 11.8 seconds into the startup is the second torsional resonance at 3,260 CPM. The first torsional resonance, at 1,275 CPM, is encountered at 14.5 seconds into the startup. Figure 33 is the animated mode shape of the first torsional resonance. All of the twist amplitude is between the motor and the bull gear. This is where the maximum shear stresses will occur. For this reason the coupling flanges on both the motor and the bull gear were made integral with the shafts. This avoids any stresses associated with shrunk-on hubs or keyways. Figure 34 shows the second animated torsional mode shape. Here there is twist across both couplings. In both these figures, for visual enhancement, the relative twist amplitude is referenced to the compressor speed. The low speed twist amplitudes are actually reduced by the gear ratio value. Figure 35 is a plot of the alternating shaft shear stresses in the motor during a portion of the startup. Figure 36 shows the maximum high speed shaft shear stresses same time period.

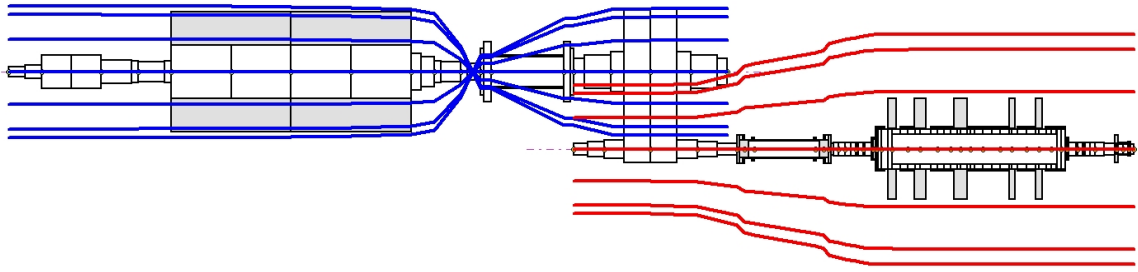


Figure 33 - First Torsional Resonance Mode Shape for Example 3 - 1,275 CPM

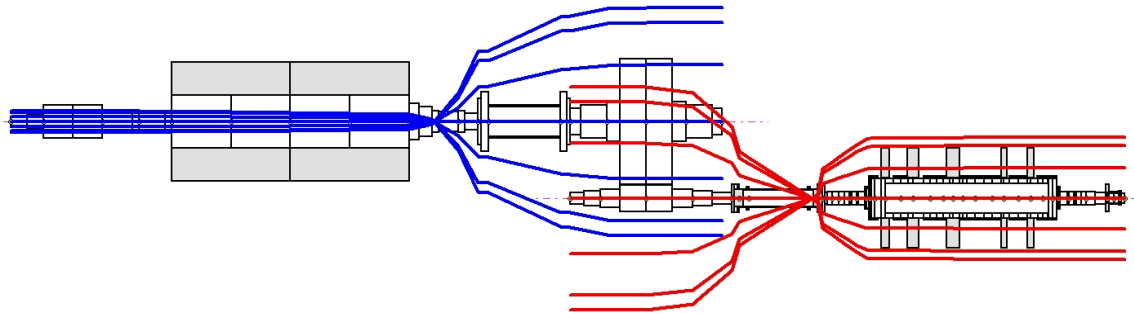


Figure 34 - Second Torsional Resonance Mode Shape for Example 3 - 3,260 CPM

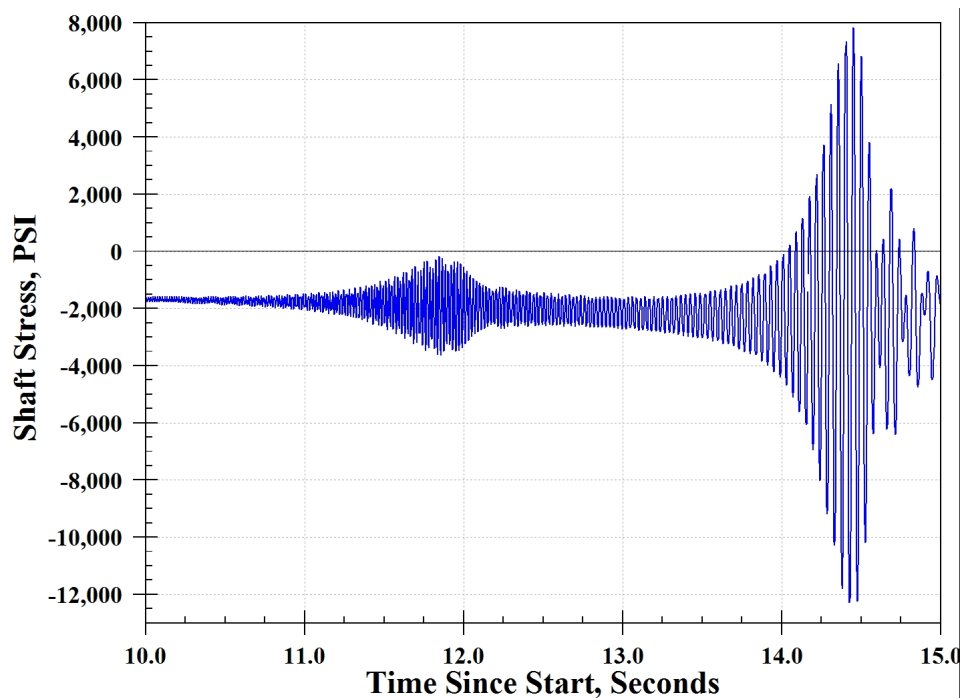


Figure 35 - Maximum Low Speed Shaft Stresses During Example 3 Startup

Due to the presence of driving torque, figure 35 shows the shear stresses offset below zero by the amount of the steady torque. The second torsional resonance reaches a maximum of 1,400 PSI, peak at about 11.8 seconds. The first torsional resonance with 10,000 PSI, peak is much more severe around 14.5 seconds.

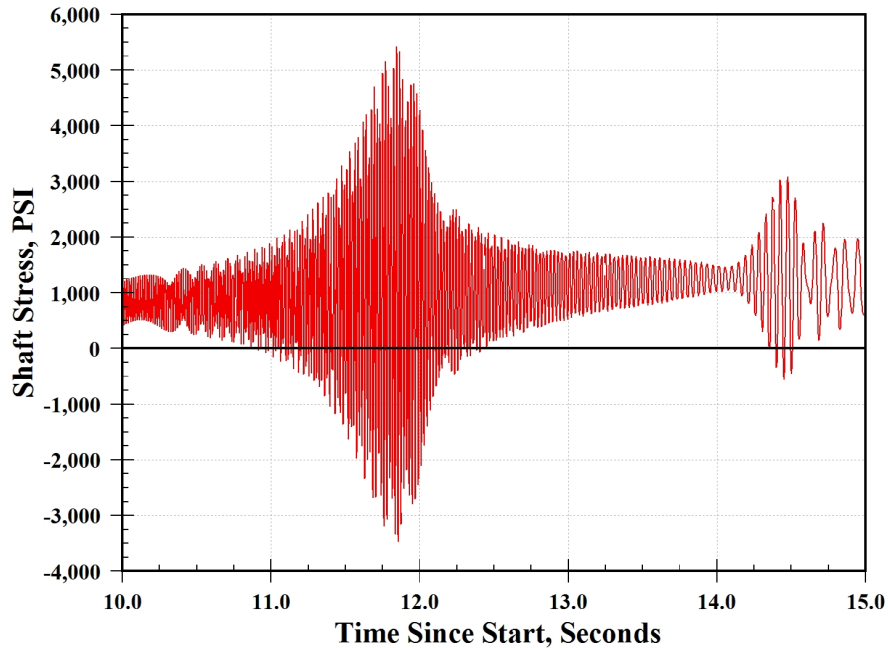


Figure 36 - Maximum High Speed Shaft Stresses During Example 3 Startup

Figure 36 is similar but with the second torsional resonance producing 4,500 PSI, peak shear stress and the first torsional resonance only 1,800 PSI, peak shear stress. This is because there is little relative twist in the high speed shafting during passage through the first torsional resonance. These plots clearly show the decreasing frequency of the torque pulsations.

It is possible to use these plots to determine the number of shear stress cycles that will accumulate and potentially fatigue the shaft. There are a number of techniques for doing this which are beyond the scope of this paper but are detailed in several of the references. The ultimate goal is infinite life but it is not unusual to settle for a finite life as long as it is economically feasible. Example 3 is a case where good design practices resulted in a machine train with an estimated 2,000 startups before a failure would occur. This train (as documented in reference 6) ran extremely smoothly for 15 years before being retired for a larger capacity unit. It is a credit to the designers that there were no problems throughout the life of the train even though the first torsional resonance at 1,275 CPM was less than 7 percent away from the 1,200 RPM operating speed.

Case 7 - Changing the System Inertia to Avoid Torsional Vibration

The fourth example involves an engine driven triplex positive displacement pump. This train is mounted on a truck and is used in the oil production industry to force large amounts of nitrogen into the earth to drive out crude oil. One pump can empty a large tank of liquid nitrogen in about 10 minutes. Figure 37 is a photograph of the truck and tank and the triplex pump. These units are in relatively severe duty and had a history of vibration and component failures. Extensive testing, covered below, revealed a torsional resonance associated with twice pump speed and three times pump speed. The 2X forcing function is generated by the universal joint driveshafts and the pump delivers 3X torque pulsations. Figure 38 is the computer model created to analyze this train. This model was simplified due to lack of specific engine, transmission, and transfer case details. The pump operating speed range is 500 to 850 RPM. The “normal” speed is 680 RPM but there are few limitations imposed on actual operation. The torsional analysis and testing revealed a train torsional resonance at 1,640 CPM. This resonance will be excited by the 2X at 820 RPM and by the 3X at 547 RPM. Strong reactions from both 2X and 3X excitations were found at up to 2 degrees peak oscillation.



Figure 37 - Truck Mounted Triplex Pump

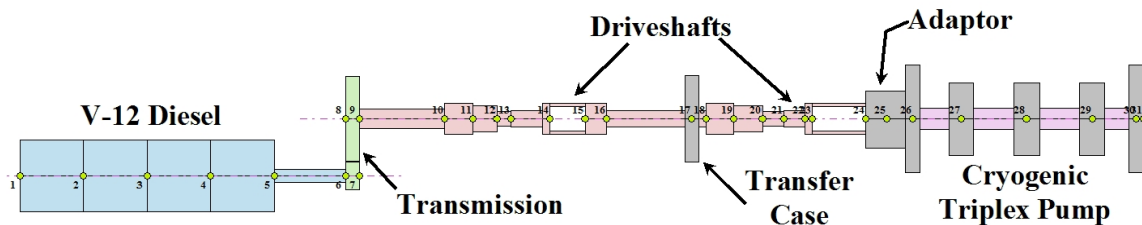


Figure 38 - Computer Model of Engine Driven Triplex Pump

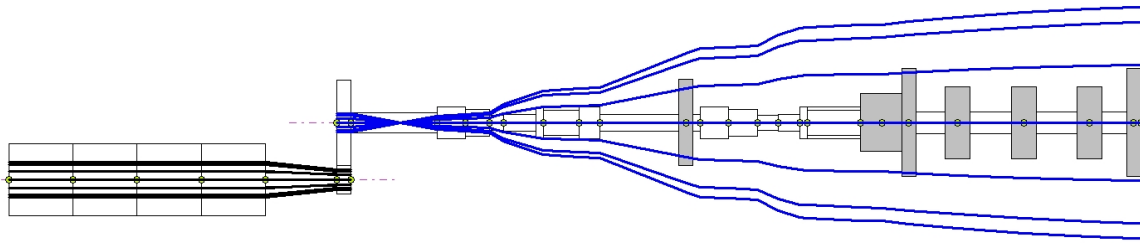


Figure 39 - Torsional Resonance Mode Shape for Example 4

The mode shape, figure 39, indicates the engine and pump are acting as rigid inertias. There were severe restrictions on the type of “fix” that could be applied to this system. First, everything had to fit in the current space. The truck could not be made longer. Stiffening the driveshafts was not possible since making them infinitely rigid would not help. Softening the driveshafts would have compromised their torque carrying capability. Most of the flexibility was in the transmission and transfer cases which could not be modified. Likewise the pump itself was not a candidate for internal change. Since the pump is acting as a rigid lumped inertia with high twist amplitude, adding inertia would lower the resonance. The adaptor between the driveshaft and the pump was increased to as large a diameter as would fit. This added about 30,000 LB-IN² to the pump inertia. Figure 40 shows the modified train.

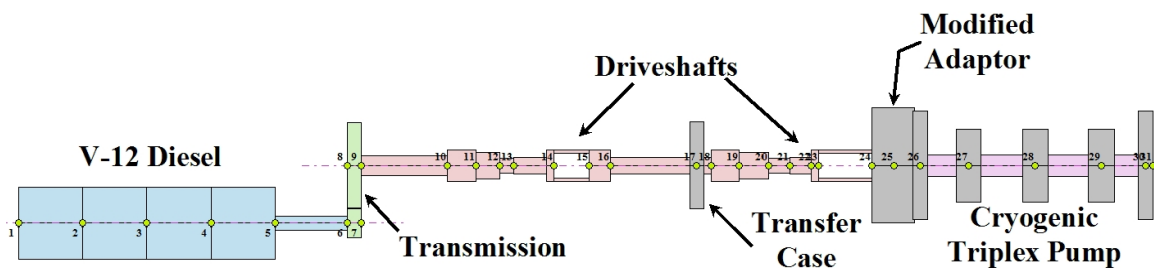


Figure 40 - Triplex Pump Train with Added Inertia

The modified system has a torsional resonance frequency of 1,080 CPM putting the 2X interference at 540 RPM and the 3X resonance at 360 RPM. Operators were cautioned against prolonged operation at these speeds. When the modified adaptor was fitted there was a dramatic decrease in vibration and over time a significant drop in failures. The experimental testing section has more details on this example.

Three of the torsional case histories have shown that systems with torsional resonance problems can be modified in several ways. The frequency of the pulsations was altered in case 4 with an impeller design change. Case 5 showed that changing the coupling stiffness is often the easiest way to shift torsional resonances. Case 6 is an example of a system that had to be designed to withstand known torsional excitations and fatigue cycles. Ideally, all machine trains should be analyzed before a significant amount of money is invested in a design. Case 7 used an inertia change to move torsional resonances away from interfering with operation.

Logically, all machine trains should be analyzed before a significant amount of money is invested in a design. It is always more expensive to retrofit a system than to have avoided the problem with good design. For example, the same company that builds the triplex pump train recently introduced a 5-cylinder quintiplex pump for delivering ever greater quantities of nitrogen. This time the torsional design was considered from the beginning and the new engine driven pumps are the smoothest ever seen in that industry.

References:

1. Nestorides, E. J., B.I.C.E.R.A. *Handbook of Torsional Vibration*, Cambridge University Press, 1958
2. Walker, Duncan N., *Torsional Vibration of Turbomachinery*, McGraw-Hill, 2003 ISBN 0-07-143037-7
3. Corbo, Mark A. And Melanoski, Stanley B., *Practical Design Against Torsional Vibration*, Tutorial, 25th Texas A&M Turbomachinery Symposium pp 189-222, September, 1996
4. Ker Wilson, W., *Practical Solution of Torsional Vibration Problems*, Volumes 1 through 5, John Wiley & Sons, 1959
5. *Tutorial on the API Standard Paragraphs Covering Rotor Dynamics and Balancing: An Introduction to Lateral Critical and Train Torsional Analysis and Rotor Balancing*, API Publication 684, February, 1996
6. Jackson, C. And Leader, M.E., *Design and Commissioning of Two Synchronous Motor-Gear-Air Compressor Trains*, 13th Texas A&M Turbomachinery Symposium, November, 1983.
7. API 613, 5th Edition, "Special Purpose Gear Units for Petroleum, Chemical, and Gas Industry Services", American Petroleum Institute.
8. Holdrege, J., Subler, W., and Frasier, W., "AC Induction Motor Torsional Vibration Consideration – A Case Study", IEEE Transactions on Industry Applications, Vol. 1A-19, No.1, Jan/Feb 1983.
9. Simmons, H. and Smalley, A., "Lateral Gear Shaft Dynamics Control Torsional Stresses in Turbine Driven Compressor Train", ASME paper 84-GT-28 presented at the 29th International Gas Turbine Conference and Exhibit, June 1984.
10. Vance, J. and French, R., "Measurement of Torsional Vibration in Rotating Machinery", ASME paper 84-DET-55 presented at the Design Engineering Technical Conference, June 1984.
11. Simmons, H, and Smalley, A., "Effective Tools for Diagnosing Elusive Turbomachinery Dynamics Problems in the Field", ASME paper 89-GT-71 presented at the Gas Turbine and Aeroengine Congress and Exhibition, June 1989.
12. Dashefsky, G.J., "The Elimination of Torsional Vibration," The third national meeting of the Oil and Gas Power Division of ASME, Penn State College, June 14, 1930.
13. Chen, W. J., and Gunter, E. J., "Introduction to Dynamics of Rotor Bearing Systems", Trafford Publishing, ISBN 1-4120-5190-8, 2005
14. Leader, M. E., "Understanding Journal Bearings", Vibration Institute, Annual Meeting, 2001.
15. Leader, M. E., "Practical Rotor Dynamics", Vibration Institute, Annual Meeting, 2002.
16. Lund, J. W., "Modal Response of a Flexible Rotor in Fluid-Film Bearings", ASME 73-DET-98, Cincinnati, September, 1973.

AMDC Rotordynamics Services

- Finite Element Analysis with advanced DyRoBes Software
- Multi-level models with realistic elements
- Complete control of foundation and support characteristics
- Any realistic type of bearing can be analyzed including gas bearings
- Seals and labyrinth effects easily included in model
- Finest output graphics available - 3D Animated graphics included
- Easy to understand reports
- Focus on Practical Solutions to machinery vibration problems

Critical Speed Analysis

Critical Speed Maps

Critical Speed Mode Shapes

Bearing and Seal Geometry and Coefficient Analysis

Squeeze Film Damper Analysis

Unbalance Response Analysis

Response to Misalignment or any other Definable Rotor Force

Harmonic Analysis (any sub or super harmonic - .237X, ½X, 2X, 2.5X, 5X, etc.)

Time Transient Analysis - Example: Sudden Blade Loss

Rotor Stability - Full API 684 Analysis

Torsional Undamped Critical Speed Analysis

Torsional Interference Diagrams

Torsional Undamped Critical Speed Mode Shapes

Torsional Damped Forced Response Analysis including Reciprocating Pulsations

Synchronous Motor Startup Simulation

Shaft Stress and Fatigue Life Calculations (Safe Number-of-Starts)